Operational Analysis of a Quantum Dot Optically Gated Field-Effect Transistor as a Single-Photon Detector

Eric J. Gansen, Mary A. Rowe, Marion B. Greene, Danna Rosenberg, Todd E. Harvey, Mark Y. Su, *Member, IEEE*, Robert H. Hadfield, Sae Woo Nam, *Member, IEEE*, and Richard P. Mirin, *Senior Member, IEEE*

***Abstract*—We report on the operation of a novel single-photon detector, where a layer of self-assembled quantum dots (QDs) is used as an optically addressable floating gate in a GaAs/$Al_{0.2}Ga_{0.8}As$ δ-doped field-effect transistor. Photogenerated holes charge the QDs, and subsequently, change the amount of current flowing through the channel by screening the internal gate field. The photoconductive gain associated with this process makes the structure extremely sensitive to light of the appropriate wavelength. We investigate the charge storage and resulting persistent photoconductivity by performing time-resolved measurements of the channel current and of the photoluminescence emitted from the QDs under laser illumination. In addition, we characterize the response of the detector, and investigate sources of photogenerated signals by using the Poisson statistics of laser light. The device exhibits time-gated, single-shot, single-photon sensitivity at a temperature of 4 K. It also exhibits a linear response, and detects photons absorbed in its dedicated absorption layer with an internal quantum efficiency (IQE) of up to (68 $\pm$ 18)%. Given the noise of the detection system, the device is shown to operate with an IQE of (53 $\pm$ 11)% and dark counts of 0.003 counts per shot for a particular discriminator level.**

***Index Terms*—Field-effect transistor (FET), quantum dots (QDs), quantum optics, single-photon detector (SPD).**

I. Introduction

TODAY'S growing interest in transmitting and processing quantum information in the form of single photons has tightened the requirements of single-photon detectors (SPDs) and driven the development of new detector technologies with diverse functionalities. Fast, low jitter SPDs that operate with high detection efficiency and low dark counts at wavelengths beyond those possible with Si avalanche photodiodes (APDs) are needed to increase the data rates and extend the link lengths of deep space transmission [1] and quantum key distribution (QKD) [2] systems. The desire to develop SPDs with high detection efficiency and low noise is further motivated by the prospect of making a loophole-free measurement of Bell's inequalities [3]. Such improvements will also impact scientific research in the areas of medical diagnosis and imaging, light detection and ranging (LIDAR) [4], and low light measurements in astronomy and chemistry. Furthermore, the development of more advanced quantum communication schemes requires SPDs with more sophisticated capabilities. For example, the realization of quantum repeaters [5] based on teleportation [6] requires the storage of quantum information. Electron spin is one possible candidate for quantum storage, motivating interest in detection mechanisms that can preserve the spin information of the photogenerated carriers.

Researchers are exploring a number of different technologies in pursuit of higher functioning SPDs, each with advantages that can be exploited for particular applications. However, most of the research is focused on methods of detection, where any information carried by the spin of the photoexcited carriers is lost during the detection process. One such class of SPDs makes use of multiplication processes to produce the gain needed for detecting individual photons. SPDs in this category include traditional photomultiplier tubes (PMTs) and APDs as well as more novel visible light photon counters (VLPCs) [7]. VLPCs exhibit high detection efficiency and photon-number-resolving capabilities not offered by traditional APDs; however, they are Si-based devices, and are therefore, appropriate for detecting photons only in the visible spectrum. InGaAs APDs [8], [9] suitable for operation at telecommunication wavelengths are commercially available; however, they exhibit higher dark counts and lower detection efficiencies than do their Si predecessors. Also, they suffer from afterpulsing that dictates that they be operated with long deadtimes.

Superconducting detectors represent another class of SPDs and are particularly well suited for operating at telecommunications wavelengths. These devices take advantage of the sensitivity of low-temperature superconducting materials to tiny changes in temperature. One type of SPD in this classification, commonly referred to as a superconducting SPD (SSPD) [10]–[12], utilizes a thin niobium nitride (NbN) wire that is current biased just below its critical temperature and embedded in a transmission line. In this device, an incident photon creates a local hotspot that quenches the superconductivity of the wire in the area of incidence and induces a high-speed voltage pulse to propagate in the transmission line. SSPDs are

Manuscript received January 15, 2007; revised June 13, 2007. This work was supported in part by the Disruptive Technologies Office (DTO).

E. J. Gansen, M. A. Rowe, M. B. Greene, T. E. Harvey, S. W. Nam, and R. P. Mirin are with the Optoelectronics Division, National Institute of Standards and Technology, Boulder, CO 80305 USA (e-mail: gansen@boulder.nist.gov; mrowe@boulder.nist.gov; mgreene@boulder.nist.gov; harvey@boulder.nist.gov; nams@boulder.nist.gov; mirin@boulder.nist.gov).

D. Rosenberg is with the Applied Modern Physics Group, Los Alamos National Laboratory, Los Alamos, NM 87545 USA (e-mail: rosenberg@lanl.gov).

M. Y. Su was with the National Institute of Standards and Technology, Boulder, CO 80305 USA. He is now with Oerlikon Optics, Golden, CO 80403 USA (e-mail: mark.su@oerlikon.com).

R. H. Hadfield was with the National Institute of Standards and Technology, Boulder, CO 80305 USA. He is now with the Department of Physics, Heriot-Watt University, Edinburgh EH14 4AS, U.K. (e-mail: r.h.hadfield@hw.ac.uk).

Digital Object Identifier 10.1109/JSTQE.2007.902843

attractive for high-speed applications and have been shown to operate at gigahertz count rates [11] with low dark count probability and timing jitter [11], [12]. Another type of superconducting detector is the transition-edge sensor (TES) [13], [14]. Here, tungsten is cooled below its superconducting temperature while a voltage bias holds the electrons in the material at the edge of the superconducting-to-normal transition. A slight change in temperature induced by the absorption of a photon modulates the resistance of tungsten, resulting in a current change for the detector. TESs are highly efficient (89% system efficiency has been demonstrated at 1550 nm [14]), and exhibit excellent photon-number resolution in both the visible and infrared spectra. The detection mechanisms used for the superconducting detectors are fundamentally different from the multiplication processes used for APDs, PMTs, and VLPCs; however, like those devices, the original photoexcited carrier is not accessible after the detection process, precluding the retrieval of any information carried by its spin.

By contrast, a less destructive method for detecting single photons has recently emerged that makes use of photoconductive gain [15] associated with persistent, three-dimensional, confinement of carriers in semiconductor diodes and field-effect transistors (FETs). Here, photogenerated carriers are safely confined in storage centers that function as optically addressable floating gates for the devices. The sensitivity of the detection process relies on a single trapped carrier influencing the transport of many (in the form of a macroscopic current) by screening the internal gate field or through Coulombic interactions between carriers. One of the potential advantages of this method of detection is that the gain mechanism may be gentle enough to preserve the spin state of the photoexcited carrier. One such SPD utilizes a layer of quantum dots (QDs) embedded in a resonant tunneling diode [16]. Photoexcited carriers trapped in the QDs shift the energy levels that mediate resonant tunneling through the barrier of the diode, and are subsequently, monitored as a change in the tunnel current. Other SPDs, based on FETs, utilize a transverse current flowing in a two-dimensional electron gas (2DEG) to monitor the trapped photocharge. The charge storage needed for these detectors has been accomplished in a number of different ways. In one case [17], naturally occurring defect centers in AlGaAs were used to store photogenerated holes, while other approaches [18], [19] utilize artificial electron traps produced by surface-mounted electrostatic metal gates. In addition, other detector designs take advantage of today's advanced epitaxial-growth-techniques-and-imbed-storage-centers-directly-into-semiconductor heterostructures in the form of self-assembled QDs [20], [21]. Constructing the SPDs in this way allows for independent control of the location of the storage centers and the location and thickness of the absorbing region of the devices. In addition, the scalability of self-assembled QD ensembles enables the fabrication of detectors with varying active area sizes and dimensions.

Recently, we reported on a quantum dot, optically gated, field-effect transistor (QDOGFET) [21] that is specially designed to efficiently trap photogenerated holes in a layer of self-assembled QDs. In this device, high internal quantum efficiency (IQE) (defined as the fraction of photons deposited in the absorption region that are counted) is achieved by designing the structure so that the internal gate field funnels the holes excited in the absorption layer to the QDs. We demonstrated that (68 ± 18)% of the photons deposited in the absorbing region are detected and that the device exhibits single-shot, single-photon sensitivity; a linear response to average number of absorbed photons; and can operate with low dark counts. In this paper, we further study the storage, persistent photoconductivity, and reset mechanisms involved in the operation of the QDOGFET, and explore the sources of secondary photogenerated signals that can contaminate the response of the detector. Using what we learn about the photoresponse of the structure, we suggest ways to increase the overall detection efficiency of the device and to improve the detector's ability to resolve the number of photons in an optical pulse.

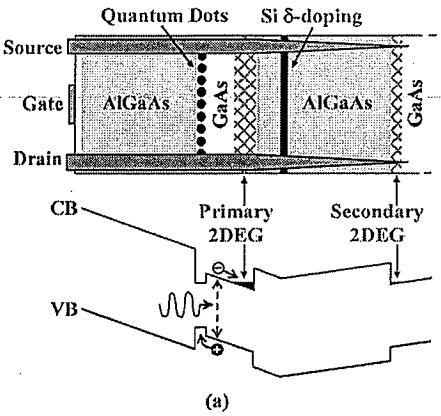

Fig. 1. (a) Schematic diagrams of the composition and band structure of the QDOGFET. CB and VB denote the conduction and valence bands, respectively. (b) SEM image of a QDOGFET where the channel width and gate length dimensions of the active area are 3.9 and 0.7 μm, respectively.

II. Construction and Principles of Operation

The QDOGFET structure is illustrated in Fig. 1. Devices were fabricated from semiconductor heterostructures grown by molecular beam epitaxy on GaAs substrates. The heterostructure layers consist of a 200-nm GaAs buffer layer, a 500-nm $Al_{0.20}$ $Ga_{0.80}$ As layer, a Si δ-doped ($\sim 1 \times 10^{12}$ cm^{-2}) layer, a 70 nm $Al_{0.20}$ $Ga_{0.80}$As layer, a 100-nm GaAs absorbing layer, an InGaAs QD layer, a 200-nm $Al_{0.20}$ $Ga_{0.80}$As layer, and a 10-nm

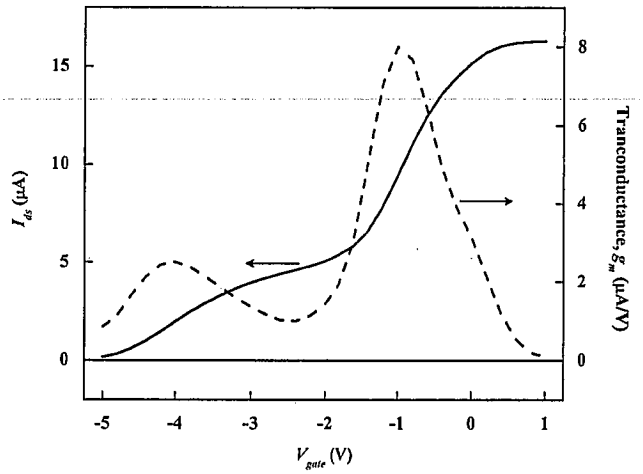

Fig. 2. $I_{\rm ds}$ of QDOGFET as a function of $V_{\rm gate}$ for a fixed 2 V bias applied across the channel and a 100-kΩ load resister wired in series with the channel. The derivative of the current with respect to the gate voltage (dashed curve) represents the transconductance g_m of the detection circuit.

n-doped ($\sim 6 \times 10^{17}$ cm^{-3}) GaAs cap layer. The growth conditions were chosen to produce a high density (400–500 μm^{-2}) of QDs, each of which is approximately 25 nm in diameter at its base. A scanning electron microscope (SEM) image of a typical device is shown in Fig. 1(b). Detectors were fabricated by depositing and annealing Ni/Au/Ge source and drain ohmic contacts on the structure surface, by etching a channel mesa between the ohmic contacts, and by depositing a 4-nm-thick semitransparent Pt Schottky barrier gate midchannel. The photosensitive area of the detector is the gated portion of the channel mesa. We constructed detectors with various channel and gate dimensions to study the influence of the active area size on the operation of the devices, and we fabricated specific control structures to investigate secondary sources of photogenerated signals. Some of the control devices were constructed with opaque, Au-covered gates to quantify signals produced by photons absorbed in the ungated portions of the channel mesa, while other control structures were fabricated from epitaxial layers grown without QDs in order to investigate secondary trapping mechanisms.

In our QDOGFETs, the Si δ-doping provides excess electrons to the conduction band, forming a 2DEG at the interface of the GaAs absorption layer and the AlGaAs layer, along with a secondary 2DEG at the edge of the GaAs buffer layer, as illustrated in Fig. 1(a). The source-and-drain contacts provide electrical connection to the primary 2DEG; however, because the contacts reach the GaAs buffer layer as well, a parallel conduction path associated with the secondary 2DEG is also formed. The electrical characteristics of a nonilluminated QDOGFET cooled to 4 K are shown in Fig. 2. Here, the current flowing between the drain and source contacts $I_{\rm ds}$ is plotted as a function of the applied gate voltage $V_{\rm gate}$ for a fixed 2-V bias applied across the channel and a 100-kΩ load resister wired in series with the channel. Also shown is the derivative of the curve, representing the transconductance $g_m = \Delta I_{\rm ds}/\Delta V_{\rm gate}$ of the detection system. Our FETs are "normally ON" devices, where the conduction of the primary and secondary 2DEGs can be "turned OFF" by reverse biasing the gate. The two conduction paths turn off at different gate voltages, and as a result, our devices can be biased in two different regimes. One regime consists of gate biases less than approximately -2 V, where only conduction associated with the secondary 2DEG is observed. The other regime consists of gate biases >-2 V, where both conduction paths are activated. In this case, however, the conduction associated with the secondary 2DEG is largely saturated, and the transconductance of the FET is dominated by contributions from the primary 2DEG. Most of the data presented in this paper were acquired while operating the devices in this regime. Note that for many of our QDOGFETs, the transconductance associated with the secondary 2DEG is less pronounced and more favorably separated from the contributions of the primary 2DEG, as compared to the data shown in Fig. 2.

When gated such that the transconductance is dominated by the primary 2DEG, the QDOGFET design provides efficient detection of photons deposited in the GaAs absorption layer. The detection process is illustrated in Fig. 1(a). When a photon is absorbed, the photogenerated hole is swept by the internal gate field toward the QD layer, where it is trapped, while the corresponding electron is swept in the opposite direction, where it joins the primary 2DEG. Confined to a dot, the positively charged hole screens the internal field, effectively changing the gate bias by a positive amount for as long as the charge is stored in the QD. It can be shown [22] that the effective increase in the gate bias $\Delta V_{\rm gate}$ caused by the addition of $N_{\rm QD}$ positive charges to the QD plane is given by

$$\Delta V_{\rm gate} = \frac{eW}{\varepsilon' A} N_{\rm QD}. \tag{1}$$

Here, e is the elementary charge, W is the distance between the gate and the QD layer, ε' is the electric permittivity of $Al_{0.20}Ga_{0.80}As$, and A is the active area. The effective change in the gate bias is subsequently monitored as a persistent change in $I_{\rm ds}$, where in the small-signal limit

$$\Delta I_{\rm ds} = g_m \, \Delta V_{\rm gate} = g_m \frac{eW}{\varepsilon' A} N_{\rm QD}. \tag{2}$$

Over time, the charging of the QDs caused by even a single carrier results in a large change in the cumulative charge transferred in the channel (a small change in the channel current integrated over a long period of time). The photoconductive gain associated with this process makes the device very sensitive to photons deposited in the GaAs absorbing layer. While the storage time of self-assembled QDs can be quite long [23], the detector can be reset electrically by temporarily forward biasing the gate. This floods the QDs with excess electrons that subsequently recombine with the trapped holes, leaving the QDs empty.

III. Charge Storage and Persistent Photoconductivity

We investigated the operation of our QDOGFET detectors by illuminating the devices with laser pulses and by performing time-resolved measurements of $I_{\rm ds}$ and of the photoluminescence emitted from the QDs. In Figs. 3 and 4, we show the results of measurements where we illuminated a device with a

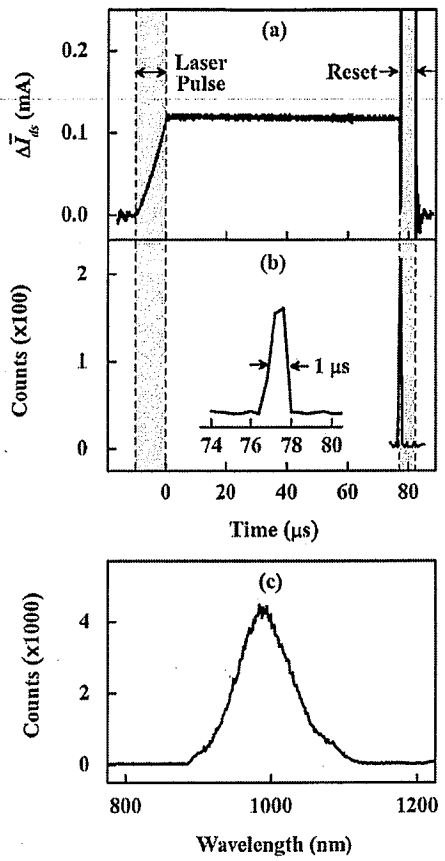

Fig. 3. Time-resolved measurements. (a) $\Delta\bar{I}_{\rm ds}$. (b) Photoluminescence emitted from the QDOGFET for $V_{\rm gate} = -1$ V under illumination with 10-μs laser pulses. The device was reset 77 μs after each laser pulse by forward biasing the gate for 5 μs. Measurements are averaged over many laser repetitions. The temporal dynamics of the photoluminescence are shown on an expanded scale in the inset. (c) Spectrum of the photoluminescence.

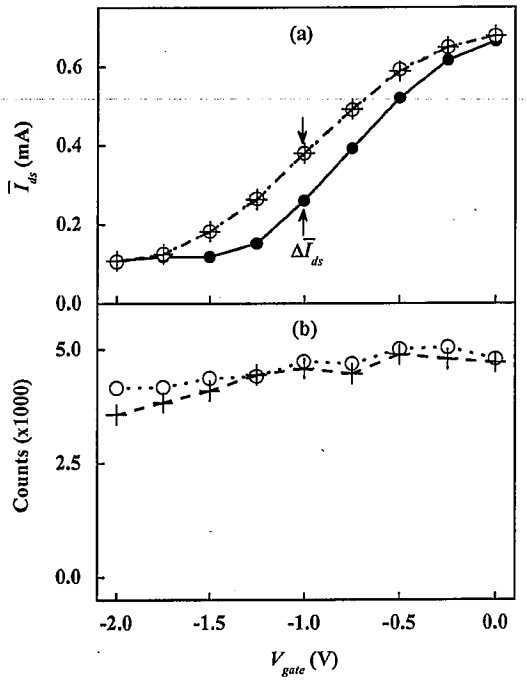

Fig. 4. (a) $\bar{I}_{\rm ds}$ measured prior to illumination (solid circles) and measured 5 μs (open circles) and 40 μs (crosses) after illumination for selected gate biases $V_{\rm gate}$. The device was reset 77 μs after each 10-μs laser pulse by forward biasing the gate for 5 μs. (b) Time-integrated photoluminescence emitted from the QDs at the time of reset, where the device was reset 5 μs (open circles) and 40 μs (crosses) after illumination. All measurements were averaged over many laser repetitions.

relatively large photosensitive area (94 μm $\times$ 3 μm) with a train of 10-μs laser pulses at a repetition rate of 10 kHz. We used a large-active-area detector and relatively high photon-flux laser pulses (thousands of photons per pulse incident on the active area) for these measurements in order to produce a measurable quantity of photoluminescence. The laser pulses were tuned (~800-nm vacuum wavelength) above the bandgap of GaAs but below the bandgap of $Al_{0.20}$ $Ga_{0.80}As$ to ensure that electron–hole pairs were generated in the GaAs absorbing layer. The QDOGFET was cooled to nominally 10 K in a liquid-helium cryostat and operated with applied gate biases between 0 and -2 V, where the transconductance was dominated by contributions from the primary 2DEG. Each laser pulse was followed by an electrical reset 77 μs later, where the gate bias was raised to $+1$ V for 5 μs.

The electrical response of the QDOGFET to laser illumination is shown in Fig. 3(a), where we plot the change in $I_{\rm ds}$ (averaged over many laser repetitions) caused by the incident laser pulses for $V_{\rm gate} = -1$ V. During laser illumination, the channel current increases linearly as photogenerated holes populate the QDs. The change in $I_{\rm ds}$ persists after illumination has ended, and shows little sign of decay over the 75 μs period shown, consistent with prolonged trapping of carriers in the dots [24], [25]. When the device is electrically reset, the channel current spikes and recovers to its preillumination value after the gate bias is returned to -1 V. As shown in Fig. 3(b), a pulse of photoluminescence is emitted from the structure at the front edge of the electrical reset when electrons flood the QDs and recombine with the trapped holes. The spectrum of the photoluminescence [Fig. 3(c)] is broad (~100 nm full-width at half-maximum) and tuned well below the laser energy and the GaAs bandgap, confirming that the photoluminescence is caused by radiative recombination of carriers in the QD ensemble. The ~1 μs duration of the photoluminescence pulse is limited by instrument resolution and dictated by the width of the temporal gate of the detection electronics used to monitor QDOGFET emission. This indicates that the QDs are discharged within the first microsecond of the electrical reset, which is consistent with the expected recombination time (typically on the order of nanoseconds) of electron–hole pairs in the QDs.

The screening of the gate field provided by the charged QDs is illustrated graphically in Fig. 4(a), where we plot $\bar{I}_{\rm ds}$ (averaged over many laser repetitions) measured prior to laser illumination and measured 5 and 40 μs after illumination for selected gate biases. The $\bar{I}_{\rm ds}$ curves obtained after illumination are shifted with respect to the curve obtained prior to illumination, indicating that the positively charged holes stored in the QDs effectively increase the gate bias of the FET, as predicted in (1). The shift

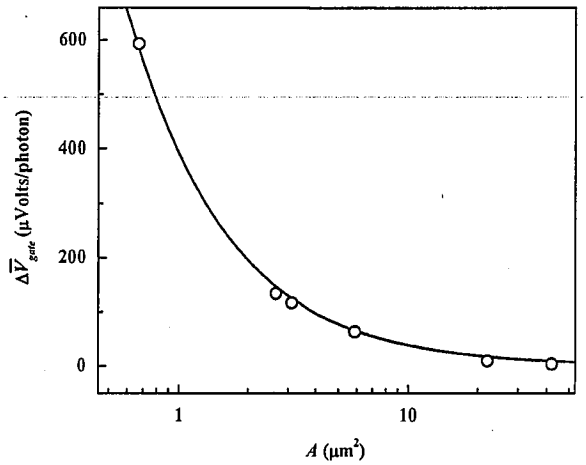

Fig. 5. Average effective change in V_{gate} per photon deposited in the GaAs absorption region versus the size of the active area A. The solid curve represents a $1/A$ fit to the data.

in the data observed at $t = 40$ μs is equal to that observed at $t = 5$ μs, demonstrating the persistence of the effect.

The time-integrated photoluminescence emitted from the QDs when the device was reset 5 and 40 μs after illumination is plotted in Fig. 4(b) for comparison. These data provide relative measures of the numbers of photogenerated holes that were stored in the QDs at the times $\bar{I}_{\text{ds}}$ was measured in Fig. 4(a). The photoluminescence emitted from the QDs has little bias dependence, indicating that approximately the same numbers of photogenerated holes were trapped by QDs for each of the gate biases shown. Also, there is little change in the amount of photoluminescence emitted from the dots at $t = 40$ μs as compared to $t = 5$ μs, verifying that the trapped holes were effectively stored in the dots for each of the selected gate biases.

The data shown in Fig. 4 illustrate that although holes are confined to the QDs over the entire range of gate voltages shown, the electrical readout of that trapped charge in the form of ΔI_{ds} depends strongly on the applied bias. Because the charged QDs shift the $\bar{I}_{\text{ds}}$ curves with respect to V_{gate}, the maximum conversion of the trapped charge to ΔI_{ds} (in the small-signal limit) occurs for gate biases where the transconductance is optimized, in accordance with (2).

Equation (2) indicates that ΔI_{ds} is inversely proportional to the area of the photosensitive region. We investigated this dependence by performing measurements on a number of different devices with varying active areas. The results of these measurements are shown in Fig. 5. Here, we plot the average change in the gate voltage ($\Delta\bar{V}_{\text{gate}} = \Delta\bar{I}_{\text{ds}}/g_m$) per absorbed photon in order to negate the variation in the transconductances of the devices used in the study. The data confirm the $1/A$ dependence of $\Delta\bar{V}_{\text{gate}}$ predicted by (1).

IV. Analysis of Photoresponse

In this section, we show that the persistent photoconductivity exhibited by our QDOGFETs can be used as a very sensitive means of detecting photons, and we explore the various ways photogenerated signals are produced in the structures. The devices used in these studies have active areas of dimensions 3.9 μm × 0.68 μm, which yield larger single-photon signals than the larger (94 μm × 3 μm active area) device discussed in Section III. The thickness (100 nm) of the absorption layer dictates that ~10% of the photons (with vacuum wavelength ~800 nm) transmitted by the semitransparent Pt gate are absorbed by this layer, while the remaining photons are deposited in the much thicker GaAs buffer layer. In addition, photons are also absorbed in the ungated sections of the channel mesa, where fringe fields that extend past the boundaries of the metallic gate expand the effective active area of the FET. Here, we use the Poisson statistics of the laser pulses along with specially designed control devices to characterize the response of the QDOGFET to carriers generated throughout the heterostructure and to evaluate the sensitivity and quantum efficiency of the detector.

We investigated the response of the QDOGFET to individual laser pulses by illuminating the device with a 0.5 Hz train of highly attenuated pulses and by monitoring the laser-induced change in I_{ds} for each shot. The device was illuminated with 20-μs laser pulses that were attenuated such that, on average, 2.2 photons were absorbed per pulse in the GaAs absorption layer beneath the Pt gate (denoted by $\bar{N}_{\text{abs}}$), while 21 photons were absorbed per pulse in the gated GaAs buffer layer (denoted by $\bar{N}_B$). The spot size (40 μm $1/e$ diameter) of the incident pulses was kept large enough to provide uniform illumination of the active region. The device was reset 500 ms after each pulse by temporarily raising the gate bias to +1 V for 1 ms. Fig. 6(a) shows a typical shot acquired for $V_{\text{gate}} = -0.8$ V. Each pulse produced a persistent step in the channel current. To determine the step height for each shot, we averaged $I_{\text{ds}}(t)$ over 50 ms windows leading up to and following a 10 ms temporal gate surrounding the arrival of each laser pulse, and then, subtracted the two averaged values.

We studied the contributions of both the carriers generated in the GaAs absorption layer and the carriers excited in the thick GaAs buffer layer to the photoresponse of the detector by performing measurements over a broad range of gate biases. We plot in Fig. 6(b) the mean step height $\Delta\bar{I}_{\text{ds}}$ induced by the laser pulses as a function of V_{gate}. The transconductance of the device is also shown for comparison. Notice that laser-induced signals are produced while the gate is biased in both the regimes discussed in Section II. For $V_{\text{gate}} > -1.5$ V, the measured step heights roughly scale with the transconductance associated with the primary 2DEG, consistent with persistent trapping of photogenerated holes in the QDs. By contrast, for $V_{\text{gate}} < -1.5$ V, the observed step heights are proportional to the transconductance associated with the secondary 2DEG. These signals are also observed by the use of a nominally identical FET constructed without QDs [data shown in the inset of Fig. 6(b)], indicating that they are *not* associated with QDs.

We gain further insight into the origins of the signals produced in the two gate regimes by constructing histograms of the measured step heights and by investigating the statistics of the distributions. Fig. 7(a) shows the histograms acquired for $V_{\text{gate}} = -0.8$ V, where the transconductance of the device is dominated by contributions from the primary 2DEG, whereas

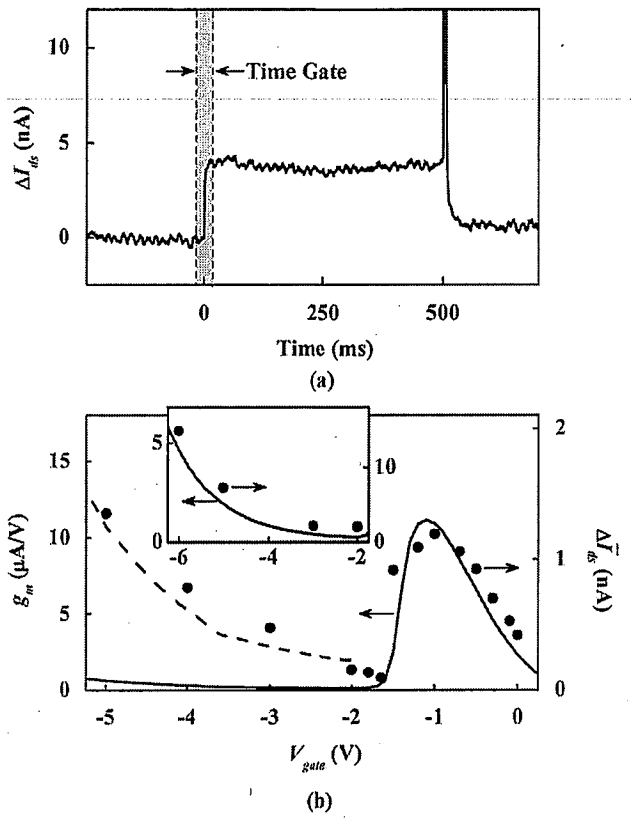

Fig. 6. (a) Single-shot measurement of the change in $I_{\rm ds}$ of a QDOGFET with a 3.9 μm × 0.68 μm active area for $V_{\rm gate} = -0.8$ V and $\bar{N}_{\rm abs} = 2.2$. (b) Transconductance g_m (solid curve) and the average change in $I_{\rm ds}$ (solid circles) of the QDOGFET measured during a 10 ms time gate surrounding the arrival of each laser pulse as a function of $V_{\rm gate}$. The dashed line represents g_m magnified by a factor of 17. (Inset) Data acquired with a nominally identical device constructed without QDs. The axes of the inset are labeled the same as in (b).

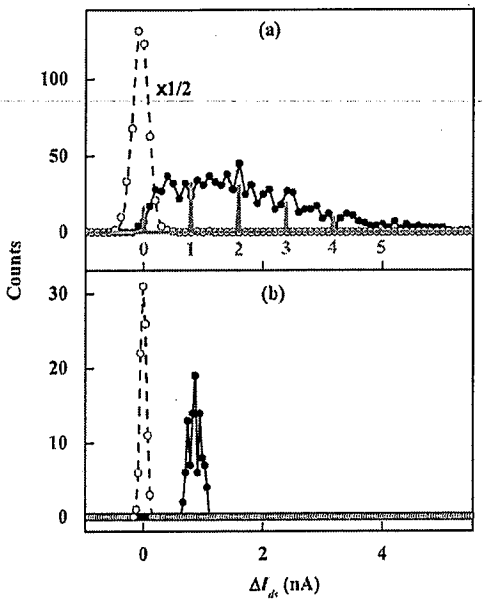

Fig. 7. Step height, $\Delta I_{\rm ds}$, distributions (solid circles) measured for $\bar{N}_{\rm abs} = 2.2$ with different values of $V_{\rm gate}$. (a) −0.8 V. (b) −3.0 V. Distributions acquired without laser illumination (open circles) are also shown for comparison. Superimposed on the data in (a) is the ideal Poisson distribution (solid gray curve) for 1.8 mean photoevents. Numbers below the curve label the individual events.

Fig. 7(b) shows data acquired for $V_{\rm gate} = -3.0$ V, where the transconductance is dominated by contributions from the secondary 2DEG. Distributions are shown both with and without laser illumination. In the absence of illumination, distributions acquired for the two biases look quite similar. In both cases, the histograms are symmetrically distributed about the origin. The peaks are well fit by Gaussian functions with full widths at the 1/e points of 0.4 and 0.1 nA for $V_{\rm gate} = -0.8$ and −3.0 V, respectively, representing current fluctuations caused by electrical noise. The fact that the peak observed in Fig. 7(b) is narrower than that observed in Fig. 7(a) can be attributed to the reduced channel current and the smaller transconductance exhibited by the device for the larger reverse bias. The former results in lower intrinsic channel noise [26] while the latter results in a lower magnification of the gate noise.

By comparison, with laser illumination, much more profound differences are observed between the distributions shown in Fig. 7 for the two gate biases. While, in both cases, histograms of laser-induced steps centered about nonzero means are observed, the statistics of those distributions are quite different. For $V_{\rm gate} = -0.8$ V, the steps are asymmetrically distributed about the mean, where the width and the mean of the distribution are comparable. By contrast, the width of the distribution acquired for $V_{\rm gate} = -3.0$ V is much narrower with respect to its mean. From these observations, and given the Poisson statistics of the laser light, we can draw conclusions about the number of photons detected for each of the two bias conditions. Neglecting noise sources within the detection system that smear out the step-height distributions produced by the Poisson source (i.e., for a perfect detector response), the mean number of photons detected per pulse is given by $(\mu/\sigma)^2$ [27], where μ and σ are the mean and standard deviation of the step-height distribution, respectively. The statistics of the distribution for $V_{\rm gate} = -0.8$ V indicate that these signals are associated with a small average number of photons [$(\mu/\sigma)^2 \sim 2$], in line with the number of photons ($\bar{N}_{\rm abs} = 2.2$) deposited in the gated portion of the GaAs absorption layer per pulse. We further illustrate this point by superimposing on the data an ideal Poisson distribution for 1.8 mean photons (the details in arriving at this mean number of photons will be discussed later in the section). Conversely, the statistics for $V_{\rm gate} = -3.0$ V (a much narrower distribution) indicate that these signals are associated with pulses of at least an order of magnitude more photons, consistent with the number of photons ($\bar{N}_B = 21$) absorbed in the gated portion of the thick GaAs buffer layer.

The observations that the signals produced for $V_{\rm gate} < -1.5$ V are persistent (lasting for over 500 ms) occur without the presence of QDs, exhibit statistics reflective of the number of photons absorbed in the buffer layer, and are proportional to the transconductance associated with the secondary 2DEG suggest that they are due to the capture of carriers in dilute traps in the GaAs buffer layer [17]. These carriers are not expected to directly affect the conduction of the

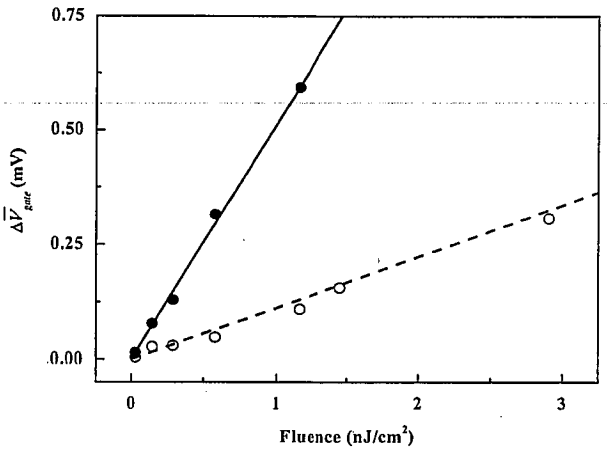

Fig. 8. Average change in V_{gate} of a 3.9 μm × 0.68 μm active area QDOGFET with semitransparent Pt gate (solid circles) and an identical device with an opaque Au gate (open circles) as a function of the pulse fluence of the incident laser light. Solid and dashed lines are linear fits to the data.

primary 2DEG due to screening by the δ-doping layer; however, they can contaminate the signals measured for $V_{\text{gate}} > -1.5$ V through a small amount of transconductance associated with the secondary 2DEG that persists in this bias regime.

In addition to exciting carriers in the GaAs buffer layer, the laser pulses also excite carriers in the ungated portion of the channel. We investigated the extent to which these carriers can change the channel conductance by performing measurements on an identical 3.9 μm × 0.68 μm active area QDOGFET that was fabricated with an opaque layer of Au on top of the Pt gate to prevent transmission. As a result, photons were absorbed only in the ungated portions of the channel. In Fig. 8, we show the laser-induced changes in the gate voltage of the QDOGFET with the opaque Au gate as compared to the changes measured with the device with a semitransparent gate for selected pulse fluences. In both cases, the devices were biased such that their transconductances were dominated by the primary 2DEG. We compare $\Delta\bar{V}_{\text{gate}}$ (as opposed to $\Delta\bar{I}_{\text{ds}}$) for the two devices in order to negate differences in the transconductances of the two structures. The data indicate that photons absorbed outside the physical gate account for ~20% of the total signal changes. By scanning the laser beam across the channel mesa, we observed that electrical signals were produced only when the channel mesa regions very close to the gate edges were illuminated, consistent with the effects of fringe fields that effectively expand the photosensitive region of the device. Because the strength of the fringe fields decay with increasing distance from the physical gate, charged QDs positioned with different proximities to the gate influence the conduction of the channel with different magnitudes. These edge effects result in nonuniformities in the signals produced by individual photons, and consequently, degrade the photon-number resolution of the detector.

By isolating the signals associated with the trapping and storing of photogenerated holes in QDs beneath the physical gate, we can determine the sensitivity of the QDOGFET to photons deposited in the GaAs absorbing region and the quantum efficiency of this detection process. The mean number of holes trapped in QDs within the active area $\bar{N}_{\text{QD}}$ can be extracted from the step-height distributions plotted in Fig. 7(a); however, in order to get an accurate value, it is important to eliminate contributions to the mean μ and standard deviation σ of the total distribution not directly related to storage of charge in the QDs under the physical gate. The measurements presented in Figs. 6–8 indicate that secondary signals associated with carriers excited in the GaAs buffer layer and in the ungated channel do contribute to the total signal changes shown in Fig. 7(a). With these effects in mind, we write μ and the variance σ^2 of the total distribution as the sums $\mu = \mu_{\text{QD}} + \mu_{\text{FF}} + \mu_B + \mu_0$ and $\sigma^2 = \sigma^2_{\text{QD}} + \sigma^2_{\text{FF}} + \sigma^2_B + \sigma^2_0$. Here, μ_0 (σ_0) is the mean (standard deviation) of the distribution acquired without illumination, and μ_{QD} (σ_{QD}), μ_{FF} (σ_{FF}), and μ_B (σ_B) are, respectively, the contributions to the mean (standard deviation) of the distribution associated with holes confined by QDs under the physical gate, holes trapped in QDs gated by fringe fields, and carriers excited in the GaAs buffer layer. Although there is some overlap between the terms associated with fringe fields and the terms associated with the carriers excited in the buffer layer, the contributions from carriers excited in the buffer layer beyond the physical gate are assumed to be small and will not be separately accounted for in this treatment.

We determine μ_0 and σ_0 from the data acquired without illumination and μ_{FF} and σ_{FF} from the data obtained with the device constructed with an opaque Au gate; however, μ_B and σ_B are more difficult to quantify for the -0.8 V gate bias used in acquiring the data presented in Fig. 7(a). Judging from the weak signals observed for $V_{\text{gate}} = -1.65$ V [Fig. 6(b)], where conduction associated with the secondary 2DEG is very small, and data collected with the device constructed without QDs [inset of Fig. 6(b)], we estimate μ_B as ~10% of the total mean μ. In addition, we assume that the contribution of $\sigma^2_B = \mu^2_B/\bar{N}_B$ to the variance σ^2 of the total distribution is negligible, as a consequence of the relatively large number of carriers excited in the buffer layer ($\bar{N}_B = 21$) that are responsible for this contribution.

Taking the secondary sources of signals into account, a calculation of $\bar{N}_{\text{QD}} = (\mu_{\text{QD}}/\sigma_{\text{QD}})^2$ for the data shown in Fig. 7(a) yields $\bar{N}_{\text{QD}} = 1.8$. Superimposed on the data in the figure is an ideal Poisson distribution for 1.8 mean photoevents. Based on this data analysis, we find that, on average, each trapped hole changes I_{ds} by 0.8 nA, denoting the spacing of the individual peaks in the ideal distribution. This value compares quite well with the expected modulation calculated from (2), where, for our experimental parameters, ΔI_{ds} caused by a single trapped hole is calculated to be 0.7 nA. The subphoton sensitivity of the QDOGFET to light absorbed in the GaAs active region is illustrated in Fig. 7(a) by comparing the single-photon peak of the ideal distribution to the width of the histogram measured in the absence of illumination. The detector is sensitive to a quarter of a photon, as defined by the ratio of the signal produced by a single photon to the half-width at the $1/e$ points of the distribution acquired without laser illumination. Although the detector is sensitive to single photons, the individual photoevents are not resolved in the data. We attribute the lack of photon-number resolution, in large part, to nonuniformities

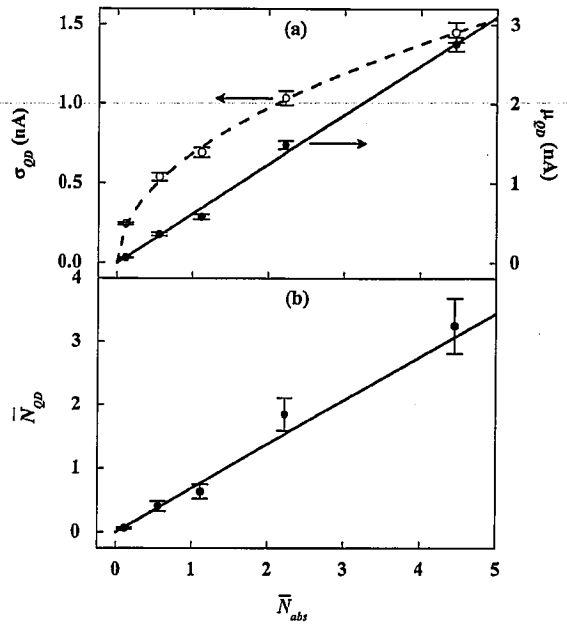

Fig. 9. (a) Parameters μ_{QD} and σ_{QD} as a function of $\bar{N}_{\mathrm{abs}}$. (b) Mean number of holes trapped by QDs, $\bar{N}_{\mathrm{QD}}$, calculated from the distribution statistics plotted in (a). The solid and dashed curves plotted in (a) and (b) represent linear and square-root fits to the data, respectively.

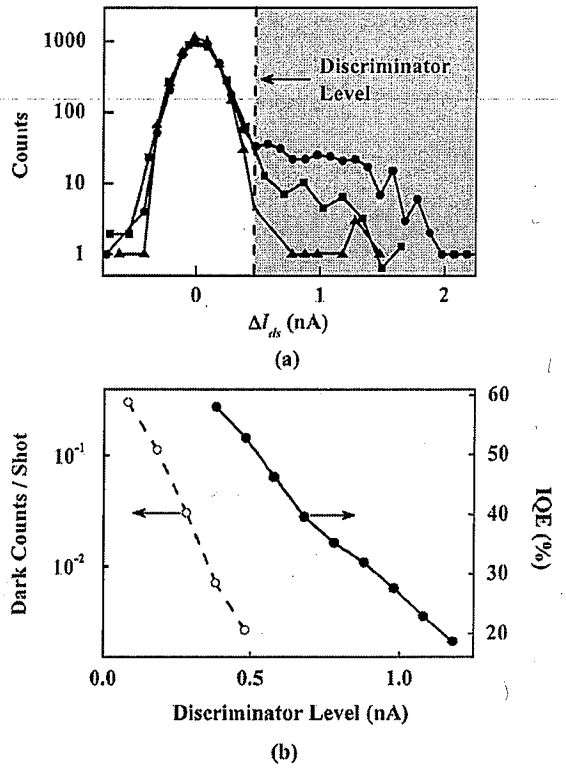

Fig. 10. (a) Step height, ΔI_{ds}, distributions acquired with a QDOGFET with a semitransparent Pt gate in the absence of illumination (triangles) and with illumination, where $\bar{N}_{\mathrm{abs}} = 0.11$ (circles), for $V_{\mathrm{gate}} = -0.8$ V. Squares denote data obtained with a QDOGFET with an opaque Au gate for the same illumination conditions as for the circles. (b) Dark counts per shot and the IQE as a function of the discriminator level. Step heights were measured during 10 ms detection windows timed with the arrival of the laser pulses.

in the step heights caused by the trapping of holes in QDs near the edges of the active area (coupled with detector noise).

The IQE of the detector denotes the fraction of holes generated in the GaAs absorption layer beneath the Pt gate that are captured by QDs. In Fig. 9, we show the quantities extracted from our measurements (conducted for a number of different incident photon fluxes) that are used to determine the IQE of the detection process. In Fig. 9(a), μ_{QD} and σ_{QD} are plotted as a function of the mean number of photons absorbed in the GaAs active region per pulse $\bar{N}_{\mathrm{abs}}$, where the vertical error bars are based on the measurement statistics. The linear and square-root dependences of μ_{QD} and σ_{QD} on $\bar{N}_{\mathrm{abs}}$, respectively, reflect the Poisson statistics of the laser pulses used in the measurements. The resulting linear dependence of $\bar{N}_{\mathrm{QD}}$ on $\bar{N}_{\mathrm{abs}}$ is illustrated in Fig. 9(b). A weighted linear fit to the values indicates that $(68 \pm 18)\%$ of the holes excited in the GaAs absorption region are trapped by QDs beneath the physical gate. The stated error includes scatter in the data as well as uncertainties in laser power, attenuation, experimental geometry, and absorption.

V. Single-Photon Detection Performance

In addition to using the Poisson statistics of the laser pulses to characterize the response of the QDOGFET, we further investigated the ability of the QDOGFET structure to detect single photons by illuminating it with very low-photon-flux pulses, where rarely was more than one photon absorbed in the GaAs active region for a given pulse. In this case, the correspondence between photocounts and trapped holes is nearly one-to-one. Results of these measurements are shown in Fig. 10(a), where step-height histograms are plotted for $\bar{N}_{\mathrm{abs}} = 0.11$ and in the absence of illumination. Also shown in the figure is the distribution of step heights obtained with the companion QDOGFET fabricated with an opaque, Au-covered gate under identical illumination conditions. The histogram obtained for the QDOGFET with a semitransparent Pt gate under illumination is composed of two main parts: a sharp Gaussian feature centered at the origin, representing current changes resulting from random noise, and a pronounced shoulder. The drastic reduction of the shoulder in the absence of the illumination indicates that it is dominated by photoinduced counts with very few dark counts. In addition, the suppression of this shoulder for the device with the opaque gate indicates that it is dominated largely by counts caused by single photons absorbed in the active region of the device.

In practice, only signal changes above a set discriminator level should be counted in order to reduce the probability of mistaking a dark count caused by noise for a real photon count. By choosing a large discriminator level, one can be assured that the measured counts are associated with photons; however, incident photons causing signals that fall below the discriminator level will not be counted, lowering the quantum efficiency of the device. We demonstrate the tradeoff between the dark counts and the efficiency of the QDOGFET in Fig. 10(b), where the IQE and the corresponding dark counts per shot (occurring within a 10 ms temporal gate), determined from the low-photon-flux data, are plotted as a function of the discriminator level. Here, the IQE of the device is evaluated by summing the photocounts

(and eliminating the counts attributed to edge effects) registered above the discriminator level and by dividing this value by $\bar{N}_{\text{abs}}$. A correction of 6% is made to the resulting values to account for the small probability of absorbing multiple photons from a given laser pulse (a consequence of the Poisson nature of the laser source). The device operates with 0.003 dark counts per shot for a discriminator level of 0.48 nA with a corresponding IQE of $(53 \pm 11)\%$. This value for the IQE, with the added constraint of the discriminator level, is to be compared with the total percentage of holes excited in the GaAs absorption region that are trapped by QDs, $(68 \pm 18)\%$, as determined in Section IV. The IQE measured with discrimination is only moderately less than the value obtained without discrimination, indicating that the detector can operate with low dark counts without dramatically reducing the efficiency of the detection process.

VI. Conclusion

In conclusion, we have investigated the operation of an SPD that uses a layer of self-assembled QDs as an optically addressable floating gate in a GaAs/$Al_{0.2}Ga_{0.8}As$ δ-doped FET. We investigated the charge storage and resulting persistent photoconductivity exhibited by the device by performing time-resolved measurements of the channel current and of the photoluminescence emitted from the QDs under laser illumination. In addition, by using the Poisson statistics of laser light, we characterized the response of the detector and explored sources of photogenerated signals. The device exhibits time-gated, single-shot, single-photon sensitivity at a temperature of 4 K. It also exhibits a linear response to the average number of absorbed photons and detects photons deposited in its absorption layer with an IQE of up to $(68 \pm 18)\%$. Moreover, measurements indicate that by choosing an appropriate discriminator level, the detector can operate with low dark counts without significantly degrading the efficiency of the detection process.

Further developments of the QDOGFET will focus on improving the overall detection efficiency and the photon-number-resolving capabilities of the device. While the internal efficiency of the current structures is quite high, the overall detection efficiency (as defined by the fraction of photons incident on the active area that are counted) of the devices is less than 2.4%, depending on the discriminator level, and is currently limited by the 38% transmission of the Pt gate and the 10% absorption of the GaAs active layer. To detect a higher percentage of the incident photons, the light needs to be more efficiently coupled to the dedicated absorption region. This should be possible by optimizing the thickness of the absorbing layer and by positioning the layer inside a resonant cavity. These modifications will also eliminate secondary signals caused by absorption of photons in the thick GaAs buffer layer. Of primary importance in realizing the photon-number-resolving capabilities predicted by (1) (i.e., $\Delta I_{\text{ds}} \sim \bar{N}_{\text{QD}}$) is improving the uniformity of photoinduced steps caused by the charging of different QDs in the ensemble. Carriers confined in QDs near the edges of the gated region undoubtedly produce highly irregular responses. By masking the edges of the active area with an opaque material, we can limit the QDs available for charge storage to those in the interior of the gated region, which are expected to provide the most uniform changes to the channel current. We will also optimize the size and aspect ratio of the photosensitive region of the detector, keeping in mind that a large active area is desired for relaxed alignment tolerances and high system efficiency.

Future work on the detectors will also include constructing structures suitable for communications wavelengths through modified material compositions and operating the devices at increased speeds. In Section III, we showed that the QDOGFET responds to both light and electrical resets on microsecond timescales. The data presented in Sections IV and V were acquired at a much slower rate (0.5 Hz) than that allowed by the detector's response time in order to maximize the signal-to-noise ratio of the measurements for our current detection circuitry. By using more sophisticated amplification techniques, much higher speeds should be possible while maintaining the single-photon sensitivity of the detector. A similar FET-based SPD has been shown to operate at 400 kHz clock rates [28] by the use of a cryogenic radio frequency amplifier. It is reasonable to expect that our device can be incorporated into such a system as well.

Finally, one of the more intriguing aspects of the QDOGFET is that the gain mechanism may be gentle enough to preserve the spin state of the photogenerated carrier confined in the QD. Although we did not explore this unique aspect of the detection mechanism in this paper, spin-preserving SPDs may play an important role in the advancement of quantum information technologies and the development of quantum networks. In the device presented here, holes excited in the absorption layer are stored in the QDs. In most semiconductor systems, conduction band electrons exhibit longer spin lifetimes than do valance band holes, and therefore, are more attractive entities for carrying spin information. In working toward constructing a spin-preserving SPD, we will investigate modified QDOGFET structures engineered to store photoexcited electrons in the self-assembled QDs.

References

[1] D. M. Boroson, R. S. Bondurant, and J. J. Scozzafava, "Overview of high rate deep space laser communications options," in *Proc. SPIE Free-Space Laser Commun. Technol. XVI*, 2007, G. S. Mecherle, C. Y. Young, and J. S. Stryjewsjki, Eds., 2004, vol. 5338, pp. 37–49.

[2] P. A. Hiskett, D. Rosenberg, C. G. Peterson, R. J. Hughes, S. Nam, A. E. Lita, A. J. Miller, and J. E. Nordholt, "Long-distance quantum key distribution in optical fibre," *N. J. Phys.*, vol. 8, pp. 193-1–193-7, Sep. 2006.

[3] P. H. Eberhard, "Background level and counter efficiencies required for a loophole-free Einstein–Podolsky–Rosen experiment," *Phys. Rev. A, Gen. Phys.*, vol. 47, pp. R747–R750, Feb. 1993.

[4] W. C. Priedhorsky, R. C. Smith, and C. Ho, "Laser ranging and mapping with a photon-counting detector," *Appl. Opt.*, vol. 35, pp. 441–452, Jan. 1996.

[5] E. Yablonovitch, H. W. Jiang, H. Kosaka, H. D. Robinson, D. S. Rao, and T. Szkopek, "Optoelectronics quantum telecommunications based on spins in semiconductors," *Proc. IEEE*, vol. 91, no. 5, pp. 761–780, May 2003.

[6] C. H. Bennett, G. Brassard, C. Crepeau, R. Jozsa, A. Peres, and W. K. Wootters, "Teleporting an unknown quantum state via dual classical and Einstein–Podolsky–Rosen channels," *Phys. Rev. Lett.*, vol. 70, pp. 1895–1899, Mar. 1993.

[7] E. Waks, K. Inoue, W. D. Oliver, E. Diamanti, and Y. Yamamoto, "High-efficiency photon-number detection for quantum information processing," *IEEE. J. Sel. Topics Quantum Electron.*, vol. 9, no. 6, pp. 1502–1511, Nov./Dec. 2003.

[8] G. Ribordy, N. Gisin, O. Guinnard, D. Stucki, M. Wegmuller, and H. Zbinden, "Photon counting at telecom wavelengths with commercial InGaAs/InP avalanche photodiodes: Current performance," *J. Mod. Opt.*, vol. 51, pp. 1381–1398, Jun. 2004.
[9] S. Cova, M. Ghioni, A. Lotito, I. Rech, and R. Zappa, "Evolution and prospectus for single-photon avalanche diodes and quenching circuits," *J. Mod. Opt.*, vol. 51, pp. 1267–1288, Jun. 2004.
[10] G. N. Gol'tsman, O. Okunev, G. Chulkova, A. Lipatov, A. Semenov, K. Smirnov, B. Voronov, A. Dzardanov, C. Williams, and R. Sobolewski, "Picosecond superconducting single-photon optical detector," *Appl. Phys. Lett.*, vol. 79, pp. 705–707, Aug. 2001.
[11] A. Korneev, P. Kouminov, V. Matvienko, G. Chulkova, K. Smirnov, M. Currie, W. Lo, K. Wilsher, J. Zhang, W. Slysz, A. Pearlman, A. Verevkin, and R. Sobolewski, "Sensitivity and gigahertz counting performance of NbN superconducting single-photon detectors," *Appl. Phys. Lett.*, vol. 84, pp. 5338–5340, Jun. 2004.
[12] M. J. Stevens, R. H. Hadfield, R. E. Schwall, S. W. Nam, and R. P. Mirin, "Quantum dot single photon sources studied with superconducting single photon detectors," *IEEE J. Sel. Topics Quantum Electron.*, vol. 12, no. 6, pp. 1255–1268, Nov./Dec. 2006.
[13] A. J. Miller, S. W. Nam, J. M. Martinis, and A. Sergienko, "Demonstration of a low-noise near-infrared photon counter with multiphoton discrimination," *Appl. Phys. Lett.*, vol. 83, pp. 791–793, Jul. 2003.
[14] D. Rosenberg, A. E. Lita, A. J. Miller, and S. W. Nam, "Noise-free high-efficiency photon-number-resolving detectors," *Phys. Rev. A, Gen. Phys.*, vol. 71, pp. 061803(R)-1–061803(R)-4, Jun. 2005.
[15] A. Rose, *Concepts in Photoconductivity and Allied Problems.* New York: Interscience, 1963, ch. 1.
[16] J. C. Blakesley, P. See, A. J. Shields, B. E. Kardynal, P. Atkinson, I. Farrer, and D. A. Ritchie, "Efficient single photon detection by quantum dot resonant tunneling diodes," *Phys. Rev. Lett.*, vol. 94, pp. 67401-1–67401-4, Feb. 2005.
[17] H. Kosaka, D. S. Rao, H. D. Robinson, P. Bandaru, T. Sakamoto, and E. Yablonovitch, "Photoconductance quantization in a single-photon detector," *Phys. Rev. B, Condens. Matter*, vol. 65, pp. 201307(R)-1–201307(R)-4, May 2002.
[18] H. Kosaka, D. S. Rao, H. D. Robinson, P. Bandaru, K. Makita, and E. Yablonovitch, "Single photoelectron trapping, storage, and detection in a field effect transistor," *Phys. Rev. B, Condens. Matter*, vol. 67, pp. 45104-1–45104-5, Jan. 2003.
[19] D. S. Rao, T. Szkopek, H. D. Robinson, E. Yablonovitch, and H. W. Jiang, "Single photoelectron trapping, storage, and detection in a one-electron quantum dot," *J. Appl. Phys.*, vol. 98, pp. 114501-1–114507-4, Dec. 2005.
[20] A. J. Shields, M. P. O'Sullivan, I. Farrer, D. A. Ritchie, R. A. Hogg, M. L. Leadbeater, C. E. Norman, and M. Pepper, "Detection of single photons using a field-effect transistor gated by a layer of quantum dots," *Appl. Phys. Lett.*, vol. 76, pp. 3673–3675, Jun. 2000.
[21] M. A. Rowe, E. J. Gansen, M. Greene, R. H. Hadfield, T. E. Harvey, M. Y. Su, S. W. Nam, and R. P. Mirin, "Single-photon detection using a quantum dot optically gated field-effect transistor with high internal quantum efficiency," *Appl. Phys. Lett.*, vol. 89, pp. 253505-1–253505-3, Dec. 2006.
[22] G. Yusa and H. Sakaki, "GaAs/n-AlGaAs field-effect transistor with embedded InAs quantum traps and its programmable threshold characteristics," *Electron. Lett.*, vol. 32, pp. 491–493, Feb. 1996.
[23] J. J. Finley, M. Skalitz, M. Arzberger, A. Zrenner, G. Böhm, and G. Abstreiter, "Electrical detection of optically induced charge storage in self-assembled InAs quantum dots," *Appl. Phys. Lett.*, vol. 73, pp. 2618–2620, Nov. 1998.
[24] A. J. Shields, M. P. O. Sullivan, I. Farrer, D. A. Ritchie, K. Cooper, C. L. Foden, and M. Pepper, "Optically induced bistability in the mobility of a two-dimensional electron gas coupled to a layer of quantum dots," *Appl. Phys. Lett.*, vol. 74, pp. 735–737, Feb. 1999.
[25] D. Heinrich, J. Hoffmann, J. J. Finley, A. Zrenner, G. Bohm, and G. Abstreiter, "Electron and hole storage in self-assembled InAs quantum dots," *Physica E*, vol. 7, pp. 484–488, 2000.
[26] J. M. Peransin, P. Vignaud, D. Rigaud, and L. K. J. Vandamme, "1/*f* noise in MODFET's at low drain bias," *IEEE Trans. Electron. Devices*, vol. 37, no. 10, pp. 2250–2253, Oct. 1990.
[27] J. W. Goodman, *Statistical Optics.* New York: Wiley, 1985, p. 472.
[28] B. E. Kardynal, A. J. Shields, N. S. Beattie, I. Farrer, K. Cooper, and D. A. Ritchie, "Low-noise photon counting with a radio-frequency quantum-dot field-effect transistor," *Appl. Phys. Lett.*, vol. 84, pp. 419–421, Jan. 2004.

Eric J. Gansen received the B.S. degree in physics and mathematics from the University of Wisconsin–La Crosse, in 1997, the M.S. degree in optical engineering from the University of Rochester, Rochester, NY, in 1998, and the Ph.D. degree in electrical and computer engineering from the University of Iowa, Iowa City, in 2004.

He is currently a National Research Council Postdoctoral Fellow in the Optoelectronics Division, National Institute of Standards and Technology (NIST), Boulder, CO, where he is currently researching semiconductor quantum-dot-based nanostructures for use as single-photon detectors and quantum memory devices. He has also researched ultrafast nonlinear phenomena in semiconductor materials and nanostructures and their applications to high-speed, all-optical, polarization switching.

Dr. Gansen is a member of the Optical Society of America.

Mary A. Rowe received the B.S. degree in physics from the California Institute of Technology, Pasadena, in 1992, and the Ph.D. degree in physics from the University of California at Berkeley, in 1999.

She was a National Research Council Postdoctoral Fellow in the Time and Frequency Division, National Institute of Standards and Technology (NIST), Boulder, CO from 1999–2002, where she researched an ion-trap-based implementation of quantum computing. In 2002, she moved to the Optoelectronics Division. She has worked in the field of fiber-optic grating-based wavelength standards, and is currently researching quantum-dot-based, single-photon detectors.

Dr. Rowe is a member of the American Physical Society.

Marion B. Greene received the B.A. degree in physics from Mount Holyoke College, South Hadley, MA, in 2000.

In June 2003, she joined the Optoelectronics Division, National Institute of Standards and Technology, Boulder, CO, where she is currently engaged in semiconductor quantum-dot-based nanostructure device design, fabrication, and research.

Danna Rosenberg received the B.S. degree in physics from Rutgers, The State University of New Jersey, New Brunswick, in 1996, and the Ph.D. degree in physics from Stanford University, Palo Alto, CA, in 2002.

She was a Postdoctoral Researcher funded by the Intelligence Community Postdoctoral Research Fellowship Program at the National Institute of Standards and Technology (NIST), Boulder, CO, where she worked on developing single-photon detectors for quantum information applications. She is currently a Technical Staff Member in the Applied Modern Physics Group, Los Alamos National Laboratory, Los Alamos, NM.

Todd E. Harvey received the B.S. degree in physics from Colorado State University, Fort Collins, in 1985, and the M.S. degree in physics from the Stevens Institute of Technology, Hoboken, NJ, in 1988.

In 1988, he joined the National Institute of Standards and Technology, Boulder, CO, where he is currently with the Optoelectronics Division, and is engaged in the epitaxial growth of quantum dots, nanowires, and other novel semiconductor heterostructures.

Mark Y. Su (M'05) received the B.S. degree in physics and the B.A. degree in mathematics from the University of Rochester, Rochester, NY, both in 1995, and the Ph.D. degree in physics from the University of California at Santa Barbara, in 2001.

From 2001 to 2007, he was at the National Institute of Standards and Technology, where he developed novel single-photon detectors based on InGaAs quantum-dot field-effect transistors, photonic crystals for enhancing light extraction from light-emitting diodes, and chirped waveguide gratings for on-chip dispersion–compensation of monolithic mode-locked semiconductor lasers. He is currently with Oerlikon Optics, Golden, CO, where he is engaged in laser development for display applications.

Robert H. Hadfield received both the B.A. and M.Sc. degrees in natural sciences (physics) in 1998 and the Ph.D. degree in materials science from the University of Cambridge, Cambridge, U.K., in 2003.

In 2003, he joined the National Institute of Standards and Technology (NIST), Boulder, CO, as a Postdoctoral Guest Researcher. In January 2007, he joined the Department of Physics, Heriot-Watt University, Edinburgh, U.K., as a Royal Society University Research Fellow. He has been engaged in the development of nanoscale Josephson junctions fabricated by focused ion beam microscope. His current research interests include fabrication, and testing and implementation of ultrafast infrared superconducting single-photon detectors for applications in quantum information.

Dr. Hadfield is a member of the American Physical Society, the Optical Society of America, and the U.K. Institute of Physics.

Sae Woo Nam (M'05) received the B.S. degree in physics and electrical engineering from the Massachusetts Institute of Technology, Cambridge, in 1991, and both the M.S. and Ph.D. degrees in physics from Stanford University, Stanford, CA, in 1999.

He is currently a Project Leader with the Optoelectronics Division, National Institute of Standards and Technology (NIST), Boulder, CO, where he is engaged in advanced metrology work. His current research interests include using superconducting detectors [transition-edge sensor (TES) and superconducting single-photon detector (SSPD)] for direct detection of photons at telecommunications wavelengths and at optical wavelengths for astronomical observations and quantum information applications.

Dr. Nam was awarded a National Research Council (NRC) Postdoctoral Fellowship at the NIST for his work on advanced applications of superconducting TES-based detectors.

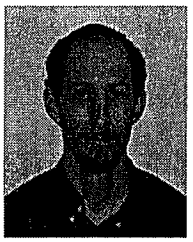

Richard P. Mirin (M'97–SM'05) received the B.S. degree from the University of California at Berkeley, in 1990, and the M.S. and Ph.D. degrees from the University of California at Santa Barbara, in 1992 and 1996, respectively, all in electrical engineering.

He is currently with the Optoelectronics Division, National Institute of Standards and Technology (NIST), Boulder, CO, where he is currently the Project Leader for the Nanostructure Fabrication and Metrology Project. The project's research is focused on precision spectroscopy of semiconductor quantum dots and the applications of quantum dots for single-photon sources and detectors. He is the author or coauthor of more than 50 papers and 80 conference presentations and proceedings.

Dr. Mirin is a member of the Optical Society of America.